2009 American Control Conference
Hyatt Regency Riverfront, St. Louis, MO, USA
June 10-12, 2009

Load Characteristics and Control of a Hybrid Fuel Cell / Battery Vehicle*

Syed Ahmed and Donald J. Chmielewski†

Abstract

The Polymer Electrolyte Membrane Fuel Cell (PEMFC) has been projected to be the fuel cell of choice for future automotive applications. Among the most challenging aspect of this application is the occurrence of severe and frequent changes in power demand. This paper will present a model aimed at mimicking the load expected in a fuel cell vehicle, including a DC motor, DC-DC converters and a rechargeable battery for peak-shaving and regenerative braking. The model also includes the kinematics of the vehicle (rotational and translational inertia as well as a simple wind resistance model), and thus can be connected to standardized drive cycle scenarios. In contrast to simple lab focused loads (resistive, constant current, constant voltage or constant power) where load impendence is directly manipulated, the manipulated variable within this load is the gain signal to the DC-DC converter. Based on this model we develop a control system architecture consisting of a number of low level regulatory loops, a power distributor for peak-shaving and finally a high level loop for tracking vehicle speed.

1. Introduction

The expected configuration of the power system within a hybrid fuel cell / battery vehicle is to combine the large energy density of an energy conversion device (a PEMFC) with the large power density of at least one energy storage device (a rechargeable battery or super-capacitor). The basic idea is that the conversion device will provide sufficient energy from a time averaged point of view, while the storage devices will deliver supplemental power during transient or peak conditions (as well as provide a mechanism for regenerative braking). Recent efforts to design control systems for this application include: Zhou et al., 2006; Vahidi et al., 2006; Thounthong et al., 2006; Zenith & Skogestad, 2007 and Kim & Peng (2007).

The size of an energy storage device indicates not only the amount of energy it can store, but also the instantaneous power it can deliver (or receive). The ratio of max power to max energy storage (usually denoted as C-rate) is a function of the specific technology. The energy conversion device is similar in the sense that max power is a function size. The main difference is that one can safely assume infinite-energy capacity. The last factor concerns the rate at which power output can be changed. Compared to the time-scale of vehicle dynamics, energy storage devices can safely change power levels nearly instantaneously. The fuel cell, on the other hand, is susceptible to sudden changes in power, as these may damage catalyst supports (Meyers & Darling, 2006; Uchimura & Kocha, 2007) or cause a flooding condition (Lauzze & Chmielewski , 2006; Ahmed & Chmielewski, 2009).

In this note we develop a simple model of the hybrid vehicle power system, and illustrate the pros and cons of various control system architectures. In the end, we propose one such architecture that exploits the power / energy density features of each device.

2. Hybrid Vehicle Model

2.1. Vehicle and Motor Models

The DC motor is governed by the following:

$$L_a \frac{di_a}{dt} = -R_a i_a - K_v \omega_o + V_a \quad (1)$$

$$J_o \frac{d\omega_o}{dt} = -\beta \omega_o + K_t i_a - T_L \quad (2)$$

where ω_o is the motor speed; i_a and V_a are the armature current and voltage; L_a and J_o are the motor inductance and inertia; β and R_a are the motor friction and internal

*Center for Electrochemical Science & Engineering Department of Chemical & Biological Engineering,Illinois Institute of Technology, Chicago, IL 60616
†Corresponding author:phone: 312-567-3537, fax: 312-567-8874, email: chmielewski@iit.edu

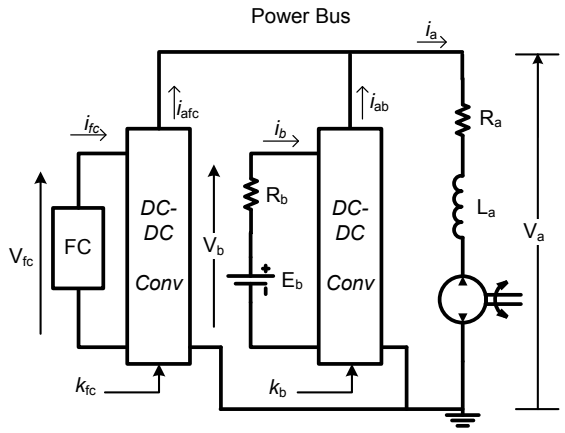

Figure 1. Power Source Connections

resistance; K_v and K_t are motor constant and T_L is the torque to motor.

The kinematics of the vehicle are modeled as:

$$M\frac{dv}{dt} = F_w - F_{drag} \quad (3)$$

$$F_{drag} = \frac{1}{2} f \rho_{air} v^2 A \quad (4)$$

where v and M are the vehicle speed and its mass; F_w and F_{drag} are the force imparted to the ground and air resistance and A, ρ_{air} and f are the frontal area, air density, and friction factor used to calculate wind resistance. Combining the two models we arrive at:

$$\frac{di_a}{dt} = \frac{1}{L_a}(-R_a i_a - K_v \omega_o + V_a) \quad (5)$$

$$\frac{d\omega_o}{dt} = \frac{1}{J_o}(-\beta_o \omega_o + K_t i_a - T_{10}) \quad (6)$$

$$\frac{d\omega_1}{dt} = \frac{-\beta_1 \omega_o + T_{10}/M_t - \frac{1}{2} f \rho_{air} A R^3 M_t^3 \omega_o^2}{(J_1 + R^2 M_t^2 M)} \quad (7)$$

$$T_{10} = K_{cl}(\omega_o - \omega_1/M_t) \quad (8)$$

$$v = R\omega_1 \quad (9)$$

where ω_1, R and J_1 are the speed of the wheel, its radius, and inertia; M_t is the gear ratio and K_{cl} is the clutch factor, (in this study K_{cl} is selected to be sufficiently large.)

2.2. The Power Source Model

The power sources are connected to the motor through a set of DC-DC converters and via a power bus. The following equations govern the battery and its DC-DC converter (see figure 1).

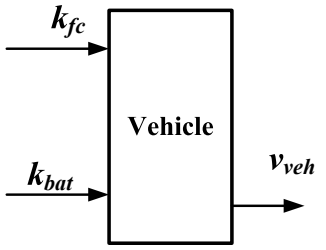

Figure 2. Open-loop plant

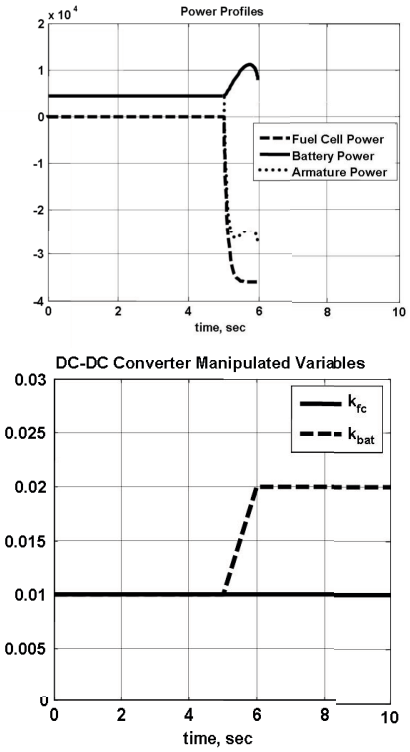

Figure 3. Open Loop Step Tests

$$V_a = k_b V_b \quad (10)$$

$$i_{ab} = i_b / k_b \quad (11)$$

$$V_b = E_b - i_b R_b \quad (12)$$

where the converter gain, k_b, will be used to manipulate the power to/from the battery. Similarly, the model for the fuel cell and its DC-DC converter is:

$$V_a = k_{fc} V_{fc} \quad (13)$$

$$i_{afc} = i_{fc} / k_{fc} \quad (14)$$

$$V_{fc} = \eta(i_{fc}) \quad (15)$$

where $\eta(i_{fc})$ is the nonlinear polarization curve of the fuel cell, which in general is a function of numerous

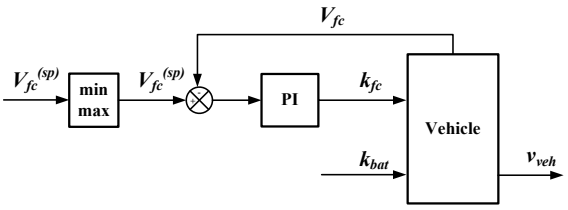

Figure 4. Fuel Cell Voltage Control

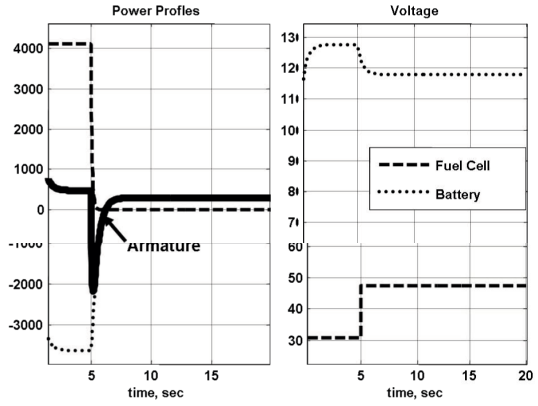

Figure 5. Fuel Cell Voltage Control Test

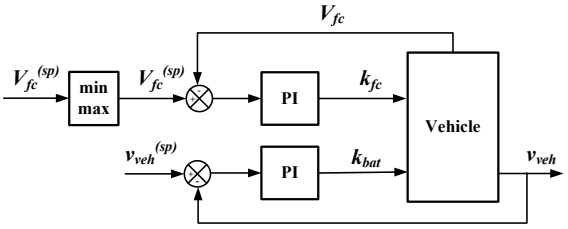

Figure 6. Single-loop speed control

operating parameters (See Lauzze & Chmielewski , 2006; Ahmed & Chmielewski, 2009). In the present study we assume the simplistic relation: $\eta(i_{fc}) = E_{fc} - i_{fc}R_{fc}$.

2.3. Open Loop Tests

Given the open loop plant of figure 2, we perform a set of step tests. However, the plot of figure 3 shows erratic behavior with regard to the fuel cell and battery power levels and in fact goes unstable after 6 seconds. In the next section, we explore the addition of a number of low level servo-loops intended to regulate the response of each.

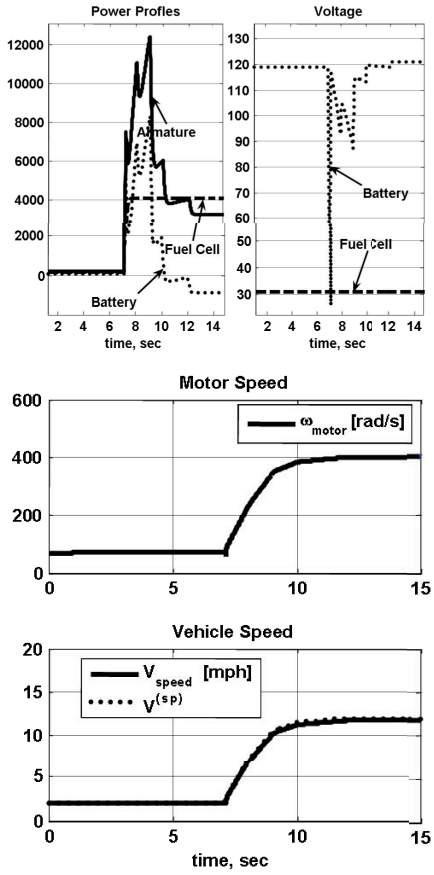

Figure 7. Single-loop speed control test

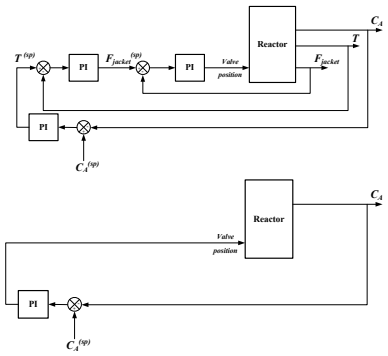

Figure 8. Lesson from Reactor Control

3. Fuel Cell/Battery Regulation

The first configuration we consider is the addition of a proportional-integral (PI) controller to manipulate the gain on the fuel cell DC-DC converter, k_{fc} (see figure 4). The max/min operator on the set-point signal is intended to block voltage requests beyond the safety limit of the fuel cell. Figure 5 illustrates the

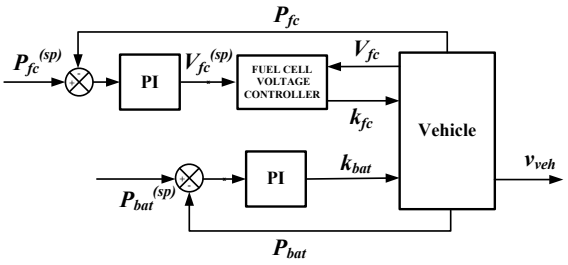

Figure 9. Power Load Control Scheme

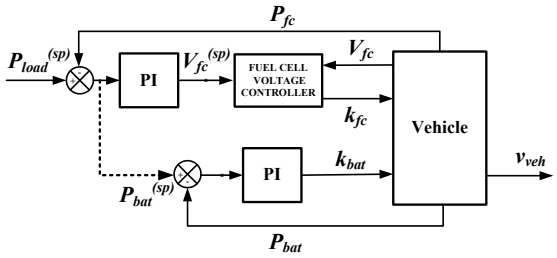

Figure 11. Power Management Controller

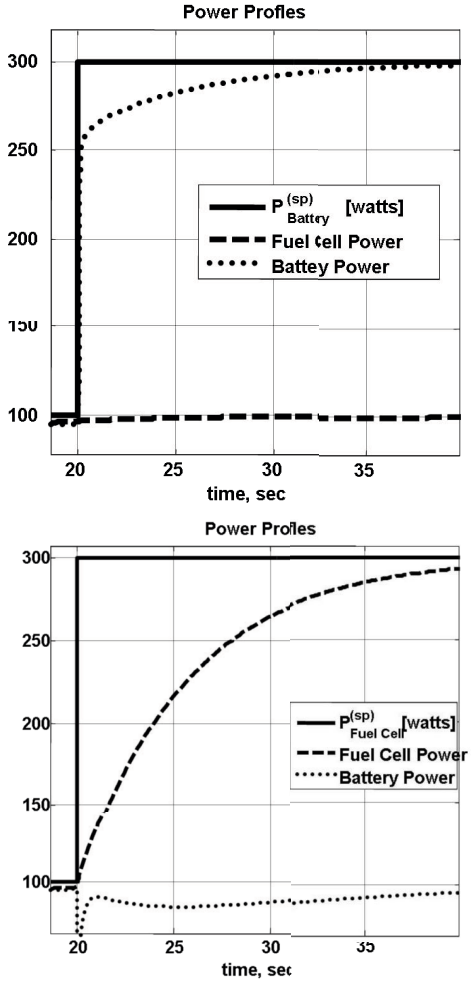

Figure 10. Power Control Tests

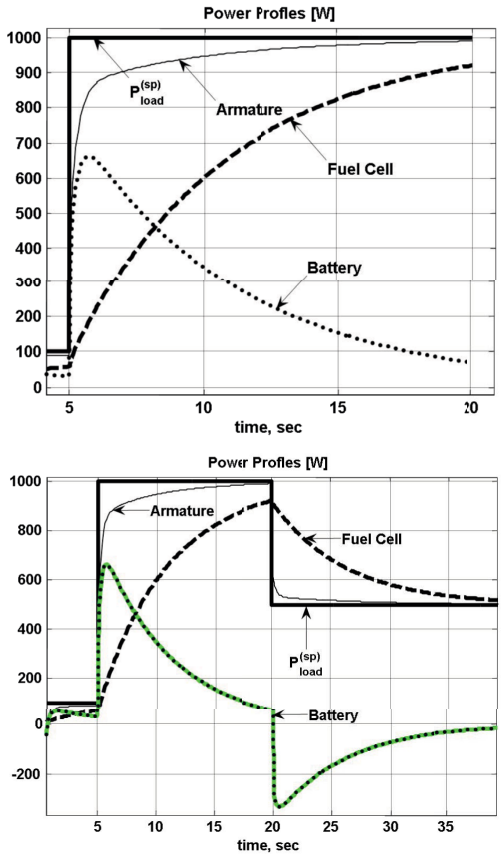

Figure 12. Hybrid Power Management Tests

response of changing $V_{fc}^{(sp)}$ from 30 to 48 and holding k_b constant. While the fuel cells acts as expected the power from the battery and thus that to the motor is dramatically influenced by $V_{fc}^{(sp)}$. To address this problem we close the loop on the battery by selecting vehicle speed as the control variable. Figure 6 illustrates the configuration and figure 7 shows the simulation results. The vehicle was maintained at 2 mph and then accelerated at a constant rate to 12 mph in 3 seconds. The simulation shows that the speed demand was met by the hybrid system, but we find that the battery is behaving erratically.

To understand the flaw of this configuration consider the following analogy of a jacket cooled exothermic reactor. A common approach to regulating exit composition is to manipulate reactor temperature via a temperature regulating loop via a jacket flow regulating loop via manipulation of valve position (see

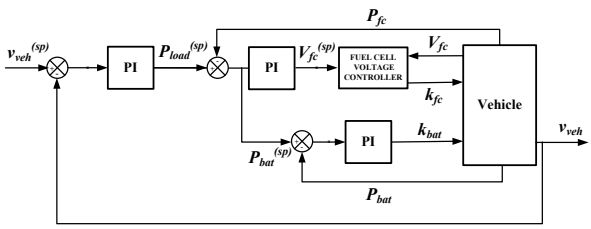

Figure 13. Speed Control

figure 8). The single-loop speed controller of figure 6 is analogous to reactor controller using a single loop to manipulate valve position. Such a configuration is certainly legitimate, but we should not expect good performance. To alleviate this problem, we add a set of power loops as indicated in figure 9. We also note that an additional inner loop for the battery could have been applied, regulating for example current. In this case, a max/min operator would have been applied to the set-point (similar to figure 4), which would block requests beyond the C-rate of the battery. The response of steps at of $P_{fc}^{(sp)}$ and $P_{bat}^{(sp)}$ show that the resulting power outputs are, for the most part, decoupled (see fig 10). The fact that these track the set-points somewhat poorly is due to the PI tuning values we selected for these loops. The motivation for these tuning choices will be discussed next.

4. Hybrid Power Management

Now that we can manipulate the power from each device somewhat independently, we turn to the more interesting question of hybrid power management. When the vehicle operator requests power to the motor, one must decide which device will deliver that power, the fuel cell or the battery. Ideally, we would like the fuel cell to respond to the average power demands while the battery covers the short term transient aspects. Using the configuration of figure 11, the step tests of figure 12 indicate just such a response. When there is a request for power, at $P_{load}^{(sp)}$, the PI of the battery power loop is tuned to respond very quickly. Then once the de-tuned fuel cell loop catches up, the battery loop will drop off. Similarly, when there is a drop in the power request, the battery will take the excess power until the fuel cell has time to respond.

Now we return to the speed control problem. Using the configuration of figure 13, figure 14 shows a much improved response as compared with figure 7.

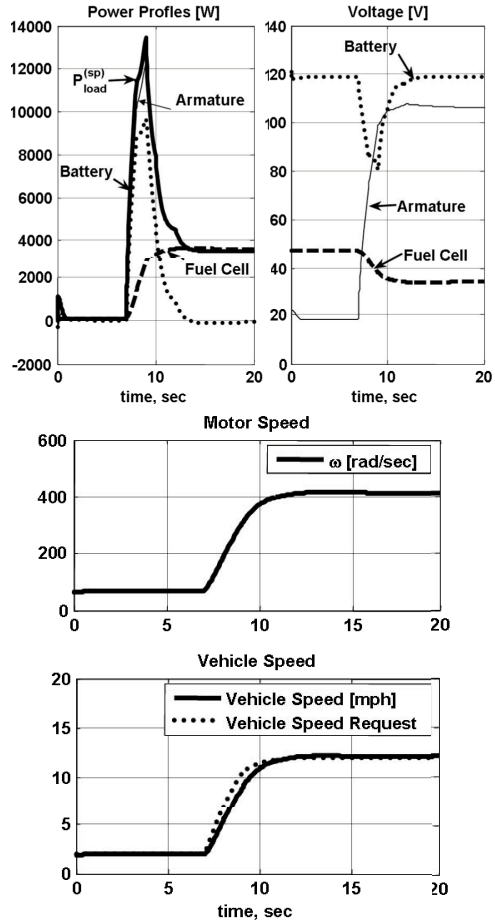

Figure 14. Speed Control Test

5. Conclusion

For the hybrid vehicle configuration of figure 1, we have concluded that a cascade control structure, containing two or three layers, can greatly improve performance and ease the task of controller tuning. At the lowest level, we advocate a voltage or current controller, similar that used in a potentiostat or galvanostat (see figure 4). While this lowest loop is optional, it has the advantage of allowing one to limit the voltage or current requests going to each device. At the second level, we propose a set of power controllers with the voltage (or current) set-points as the manipulated variables (see figure 9). At this level, the loops are tuned to account for the allowed rate of power change for each device. Specifically, the battery loop is tuned to respond quickly to power set-point changes, while that of the fuel cell is tuned to respond slowly to extend lifespan. The third level concerns power management, where figures 11 and 13 are examples of such power coordination. Future work

will focus on this area of high level controller design under the assumption of low level servo loops as a support structure.

6. Acknowledgements

This work was supported by the Department of Chemical and Biological Engineering and the Graduate College at the Illinois Institute of Technology.

7. Notation

i_a	Armature Current (A/cm^2)
V_a	Voltage (V)
ω_o	Motor Speed (rad/s)
L_a	Motor Inductance(0.06 H)
J_o	Inertia(0.10 kg-m^2)
J_1	Inertia(0.75 kg-m^2)
K_v	Motor Constant(0.25 V/rpm)
K_t	Motor Constant(0.25 V/rpm)
β_o	Motor Friction(0.004 Nm/rad-s)
β_1	Motor Friction(0.02 Nm/rad-s)
R_a	Internal Resistance(0.10 Ω)
T_L	Torque to the motor
v	Vehicle Speed (mph)
M	Mass(1000 kg)
ω_1	Speed of wheel(rad/s)
R	Radius(0.175 m)
F_w	Force to ground
F_{drag}	Air Resistance
A	Vehicle Frontal Area(1 m^2)
ρ_{air}	Air Density(1.1 kg/m^3)
M_T	Gear Ratio
f	friction factor(0.44)
K_{cl}	Clutch Factor(1000)
k_b	DC-DC Converter Gain: Battery,
k_{fc}	DC-DC Converter Gain: Fuel Cell (FC)
i_{ab}	Arm Current from Battery DC-DC Converter
i_{afc}	Arm Current from FC DC-DC Converter
V_b	Battery Voltage
E_b	Battery OC Voltage(238 V)
i_b	Battery Current
R_b	Internal Resistance(0.63 Ω)
V_{fc}	FC Voltage
E_{fc}	FC OC Voltage(95 V)
i_{fc}	FC Current
R_{fc}	Internal Resistance(0.44 Ω)

References

[1] Zhuo, J; C. Chakrabarti; N. Chang; S. Vrudhula (2006), Maximizing the lifetime of embedded systems powered by fuel cell-battery hybrids, Proc. Int. Symp. Low Pow. Elec. Des., Tegernsee, Germany, pp 424-429.

[2] Vahidi, A; A. Stefanopoulou; H. Peng (2006), Current management in a hybrid fuel cell power system: a model predictive control approach, IEEE Trans. Cont. Sys. Tech., vol 14(6) pp 1047-1057.

[3] Thounrthong, P; S. Rael; B. Davat (2006), Control strategy of fuel cell / supercapacitors hybrid power sources for electric vehicle, J. Pow. Sources, vol 158, pp 806-814.

[4] Zenith, F; S. Skogestad (2007), Control of fuel cell power output, J. Pow. Sources, vol 17, pp 333-347.

[5] Kim, M; H. Peng (2007), Power management and design optimization of fuel cell / battery hybrid vehicles, J. Pow. Sources, vol 165, pp 819-832.

[6] Meyers, J; R. Darling (2006), Model of carbon corrosion in PEM fuel cells, J. Electrochem. Soc., vol 153(8), pp A1432-A1442.

[7] Uchimura, M; S. Kocha (2007), The impact of cycle profile on PEMFC durability, ECS Trans. vol 11(1).

[8] Lauzze, K; D. Chmielewski, (2006) Power control of a polymer electrolyte membrane fuel cell, Ind. Eng. Chem. Res., vol 45, pp 4661-4670.

[9] Ahmed, S; D. Chmielewski (2009) Dynamics and control of membrane hydration in a PEMFC, Proc. Am. Cont. Conf., St Louis, MO.